INTELLIGENT WI-FI BASED CHILD PRESENCE DETECTION SYSTEM

Xiaolu Zeng[*]*, Beibei Wang*[†]*, Chenshu Wu*[⋆†]*, Sai Deepika Regani*[†] *and K. J. Ray Liu*[*†]

[*]University of Marland, College Park, MD 20742, USA.
[†] Origin Wireless Inc., 7500 Greenway Center Drive, Suite 1070, MD 20770, USA.
[⋆]The University of Hong Kong, Hong Kong, China.

ABSTRACT

Heat-stroke and death of children being left alone in a parked car has attracted more and more attentions. As a result, car manufactures start to reward solutions for in-car Child Presence Detection (CPD) system to save lives recently. However, most of the existing works rely on dedicated sensors and only achieve limited accuracy and coverage. This paper presents the first-of-its-kind intelligent CPD system using commodity Wi-Fi. Based on a statistical electromagnetic wave model to fully leverage the information in all the multipath components, the proposed CPD system mainly consists of a motion target detector to detect a child in awake/motion status, a stationary target detector to detect a sleeping child by extracting breathing rate information, and a transition target detector based on a Naive Bayes Classifier using multipath profiles as features. We build a real-time testbed and show through extensive experiments that the proposed system can achieve $\geq$ 99.34% detection rate and $\leq$ 4.38% false alarm rate, regardless of the location and motion status of a child. Built upon 2.4/5GHz Wi-Fi, the proposed system can integrate with the existing in-car Wi-Fi system with no additional hardware and calls for low CPU and memory consumptions, thus promising a practical candidate for CPD applications.

Index Terms— Intelligent child presence detection (CPD), Commercial Wi-Fi, Wireless sensing, Real-time system

1. INTRODUCTION

As reported by the *Heat Stress From Enclosed Vehicles* [1, 2], Pediatric Vehicular Heatstroke (PVH) causes an average of 38 children death and many more disabilities in the US every year. More specifically, 97% of the children reported are under the age of 6 who lack the ability to exit the vehicle on his/her own. Therefore, technological solutions are needed to monitor a child's presence in the vehicle and alert the car owner or call for emergency services. Toward this end, from 2022, the European New Car Assessment Programme (NCAP) will reward solutions of CPD Systems, which are also considered as a regulatory requirement for all newly manufactured vehicles starting from 2023 [3].

Prior works have explored different schemes for CPD application. Sensor-based CPD system requires a variety of sensors to collect the information of the child such as weight, heat [4]. Since those sensors are usually equipped on the baby seat, the coverage is limited within/next to the baby seat. Although Pyroelectric Infrared (PIR) sensor-based approach [5] extends the coverage to the Line of Sight (LOS) area with respect to the PIR sensor by detecting the motion of a child and then indicating his/her presence, PIR sensors are very sensitive to the temperature of the surroundings, which hinders its application. By incorporating with machine learning techniques [6], Vision-based CPD system [7,8] achieves very high detection accuracy while its requirement of dedicated camera to capture pictures/videos increases the cost and induces the privacy concern as well. In the last decade, Radio Frequency (RF) based in-vehicle human sensing has emerged, which can achieve CPD by detecting the vital sign or location [9, 10] of a child and becomes popular because of its superiority in preserving privacy and requiring no wearables. However, most of the RF based CPD methods rely on the millimeter wave (mmWave) signals to detect the subtle motion of a human body such as chest/heart movement (4-12mm/0.2-0.5mm), which is not available for most vehicles nowadays.

With the ubiquitous deployment of Wi-Fi on different car models [11], this paper proposes a Wi-Fi sensing based CPD system which can meet the five requirements of a typical CPD system including: 1) Entire-car Coverage, 2) Low cost, 3) Calibration-free, 4) Accurate, and 5) Responsive. We first elaborate on a statistical electromagnetic (EM) model and definition of the autocorrelation function (ACF) of the Wi-Fi Channel State Information (CSI). Based on the ACF, the proposed system presents three detectors to detect a child in different statuses: 1) a motion statistics-based **motion target detector** to detect a motion/awake child, 2) a **stationary target detector** to detect a sleeping/static child based on vital signs, and 3) a **transition target detector** using Naive Bayes Classifier to comprehensively analyze the motion statistics, vital signs and other features extracted from the CSI to identify a child in sleeping but with intermittent motion which cannot be detected by the two aforementioned detectors. By leveraging the ACF of the CSI, the proposed system harnesses

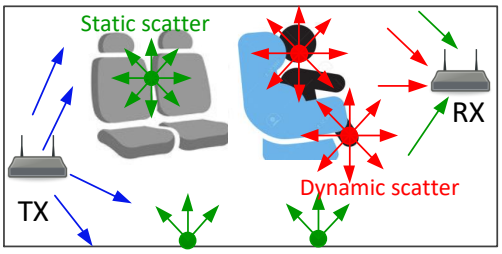

Fig. 1: Multipath propagation of the interior cabin environment.

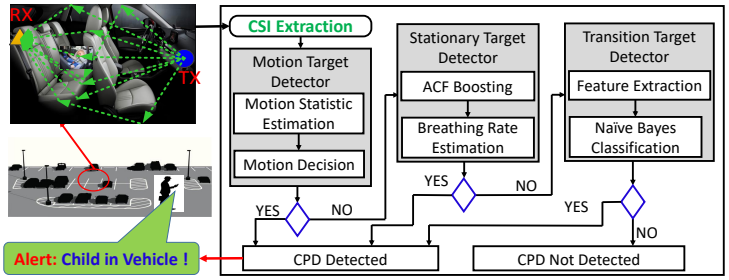

Fig. 2: System architecture.

the information contained in all the multipath components, which thus contributes to its entire-car coverage and fast response capability. We implement a testbed and extensive real-world experiments demonstrate that the proposed method can achieve $\geq 96.87\%$ detection accuracy within 20s, which outperforms the benchmark algorithms.

The rest of the paper is organized as follows. We first introduce the statistical signal model in Section 2. Section 3 presents the design of the system while Section 4 demonstrates the experiment results and real-time resource consumption. Finally, Section 5 concludes the paper.

2. STATISTICAL CSI MODEL

In a rich-scattering cabin environment as shown in Fig. 1, the transmitted signal is scattered by various scatterers and then arrives at the receiver. Based on the superposition properties of EM fields [12], the received CSI $H(t,f)$ can be modeled as the superposition of all the incoming EM waves from every individual scatterer, i.e.,

$$H(t,f) = \sum_{k\in\Omega_s(t)} s_k(t,f) + \sum_{m\in\Omega_d(t)} s_m(t,f) + n(t,f), \quad (1)$$

where $n(t,f)$ denotes the additive white Gaussian noise with power density of $\sigma_n^2(f)$ at time t and frequency f. $\Omega_s(t)$ and $\Omega_d(t)$ denote the set of static and dynamic scatterers. $s_k(t,f)$ and $s_m(t,f)$ represent the EM waves reflected by the k-th static scatterer and the m-th dynamic scatterer, respectively. As verified in [12], within a short time period, the reflection by static scatterers can be assumed stable, and $H(t,f)$ in (1) can be approximated by

$$H(t,f) \approx E_s(f) + \sum_{m\in\Omega_d(t)} s_m(t,f) + n(t,f), \quad (2)$$

where $E_s(f) = \sum_{k\in\Omega_s(t)} s_k(t,f)$ is a constant. Also, a closed vehicle can be reasonably assumed as a cavity/chamber [13], and $s_m(t,f)$ can be decomposed as a large number of plane waves with uniformly distributed arrival directions, polarization, and phases [13], i.e.,

$$s_m(t,f) = \int_0^{2\pi}\int_0^{\pi} F_m(\Theta,f)\exp(-j\vec{k}\cdot\vec{v}_m t)\sin(\alpha)\,\mathrm{d}\alpha\,\mathrm{d}\beta, \quad (3)$$

where $\vec{v}_m$ denotes the motion speed of the m-th scatter. $F(\Theta)$ denotes the complex gain from direction $\Theta = (\alpha,\beta)$ while α and β stands for the elevation and azimuth angles, respectively. $\vec{k} = -k(\vec{x}\sin(\alpha)\cos(\beta) + \vec{y}\sin(\alpha)\sin(\beta) + \vec{z}\cos(\alpha))$ and $k = \frac{2\pi f}{c}$ denote the free-space wave number with c being the speed of light.

3. DESIGN OF THE CPD SYSTEM

As shown in Fig. 2, the proposed system mainly contains a CSI extraction module followed by three different target detectors. Specifically, the *CSI extraction module* first collects CSI measurements from Wi-Fi devices which then go through a Hampel filter [14] to remove outliers caused by noise and distortions. Next, the *motion target detector* takes the preprocessed CSI to analyze the motion strength of any potential in-car target. If the motion strength is larger than a predefined threshold, the system reports a "child in vehicle". Otherwise, the *stationary target detector* is triggered to detect a child's presence if there is a continuous breathing signal in the CSI. If the decision is 'YES', "child in vehicle" is reported. If "No Presence" is reported by both the motion and stationary target detectors, the *transition target detector* will further identify if the child is in a transition status, i.e., sleeping with slight/intermittent motion. The proposed system outputs "No Presence" only when none of the three aforementioned detectors detect a child in vehicle. Next, we will introduce the details of the three detectors.

3.1. Detection of Child in Motion Status

To detect a child in motion, we consider a motion statistics firstly defined in our previous work [12] to quantify the intensity of surrounding motions for indoor scenarios based on the ACF of the CSI. We only review the key concepts of motion statistics for completeness.

Recalling (1), the ACF of CSI can be derived as

$$\rho_H(\tau,f) = \frac{E_d^2(f)}{E_d^2(f)+\sigma_n^2(f)}\rho_s(\tau,f) + \frac{\sigma_n^2(f)}{E_d^2+\sigma_n^2(f)}\delta(\tau), \quad (4)$$

where $\delta(\cdot)$ is Dirac delta function. $E_d^2(f)$ is the variance of $H(t,f)$ which measures the power reflected by all the dy-

namic scatterers. Moreover, it can be proved that $\rho_s(\tau, f)$ is a continuous function at $\tau = 0$ [15].

As a result, from (4), if there are dynamic scatterers, i.e., $E_d^2(f) > 0$, we have $\lim_{\tau\to 0} \rho_s(\tau, f) \to 1$ and

$$\lim_{\tau\to 0} \rho_H(\tau, f) = \frac{E_d^2(f)}{E_d^2(f) + \sigma_n^2(f)} > 0. \quad (5)$$

Otherwise, if there are no dynamic scatterers (i.e., no motion in surroundings), we have $E_d^2(f) = 0$ and thus

$$\lim_{\tau\to 0} \rho_H(\tau, f) = \frac{E_d^2(f)}{E_d^2(f) + \sigma_n^2(f)} = 0. \quad (6)$$

In practice, $\lim_{\tau\to 0} \rho_H(\tau, f)$ is approximated by $\rho_H(\frac{1}{F_s}, f)$ and we average the $\lim_{\tau\to 0} \rho_H(\tau, f)$ over all the subcarriers to get a more reliable motion indicator, which is called ***motion statistics*** hereafter. Given the motion statistics, the principal of the *motion target detector* is very straightforward, i.e., a child in vehicle is detected when the motion statistics is larger than a predefined threshold η_0.

3.2. Detection of Child in Static Status

Intuitively, if there is a child in static status in the vehicle, his/her vitals signs such as breathing rates (caused by chest movements) can be extracted from CSI measurements to indicate the child's presence. Although existing works have presented similar ideas for adults [16], estimating the breathing rate for a child can be more challenging because the size of a child is much smaller and his/her motion/breathing strength is much weaker than that of an adult. Therefore, we first select the top N_s (default as 10) subcarriers with the largest motion statistics[1], aiming at extracting the sucarriers which are most sensitive to the subtle chest/breathing motion. Then, a Maximal Ratio Combining (MRC) [17] scheme is leveraged to maximize the SNR of the ACF for breathing rate estimation [18]. The boosted ACF can be expressed as

$$\hat{\rho}_H^b(\tau) = \sum_{i=1}^{N_s} \omega(f_i)\rho_H(\tau, f_i), \quad (7)$$

where $\omega(f_i)$ can be viewed as the channel gain of the breathing strength on subcarrier f_i and turns out to be $\lim_{\tau\to 0} \rho_H(\tau, f_i)$ from (4). Note that we cannot maximize the breathing signal/motion directly because that the channel gain of breathing signal cannot be directly extracted from the CSI measurements. However, this problem is circumvented by applying MRC on the ACF with the motion statistics of each subcarrier as the optimal weights.

Once we get the boosted ACF $\hat{\rho}_H^b(\tau)$, the breathing rate can be estimated by $f_{\mathrm{B}} = 60/\hat{\tau}$ beats per minute (BPM) where $\hat{\tau}$ corresponds to the time lag of the first peak in $\hat{\rho}_H^b(\tau)$. Afterwards, the *stationary target detector* reports a "child in vehicle" if a normal child breathing rate (i.e., within $[6, 35]$ BPM [19]) is detected and lasts for a certain duration.

[1]Here the motion statistic is computed on each subcarrier independently.

3.3. Detection of Child in Transition Status

Although a child tends to be in either awake/motion or sleeping/static status for most of the time, empirically, there are about 6.5% time during which a sleeping child will induce slight motion such as body/hand/leg movement. In this situation, only intermittent breathing rate or motion statistics can be estimated, which cannot be detected by the motion and stationary target detectors. However, the presence of a child and his/her slight/intermittent motion can change the scatterer distribution when the signal propagates from the transmitter to receiver and thus change the angle of arrival (AoAs) [20–22] of a part of the reflected signals. The change of AoAs will further impact the multipath profile embedded in the CSI measurements. Note that it is not easy to accurately estimate the AoA change; however, such a subtle change already changes the multipath profile from the empty case. Inspired by this observation, we select the top k largest eigenvalues of the covariance matrix $\mathbf{R}_H$ calculated from the CSI after vectorization [23] as an additional feature to extract the multipath profile variation induced by the presence and motion of a child. The covariance matrix $\mathbf{R}_H$ is defined as

$$\mathbf{R}_H = \mathbb{E}[\mathbf{H}\mathbf{H}^*] \quad (8)$$

where $\mathbf{H} = [\mathbf{h}_1, \mathbf{h}_2, \cdots \mathbf{h}_Q]$, $\mathbf{h}_q = [H_{ij}(t_q, f_j)]^T$, $q = 1, 2, \cdots, Q, i = 1, 2, \cdots N_{\mathrm{A}}, j = 1, 2, \cdots, N_{\mathrm{S}}$ with $Q, N_{\mathrm{A}}, N_{\mathrm{S}}$ denoting the number of snapshot, antenna links and subcarriers, respectively. $\mathbb{E}[\cdot]$, $(\cdot)^T$, $(\cdot)^*$ represents statistical expectation, transportation and conjugate transportation. Afterwards, the motion statistics, breathing rate estimations and the top k largest eigenvalues are fused together as a new a feature vector Ψ. The *transition target detector* then leverages a Naive Bayes classifier having two classes: **empty** and **child presence** with Ψ as the input feature to identify the presence of a child. Since Naive Bayes classifier has been well studied, we omit the details in this paper and interested readers can refer to [23] and the references therein for details.

4. EXPERIMENT RESULTS

To evaluate the proposed system, we build the system using commercial Wi-Fi chipsets and the PICO-IMX7 main board running on a Linux system. We conduct extensive experiments over 20 different cars on empty data collection to evaluate the false alarm performance. We also recruit 5 children[2] aging from 4 months to 58 months including both male and female to test the CPD performance over 4 different car models. Next, we show the overall performance of the proposed system and compare it with the existing works. In addition, we show the real-time CPD and memory consumption of the proposed system to evaluate its overhead in practice.

[2]With the permission and guradinship from their parents.

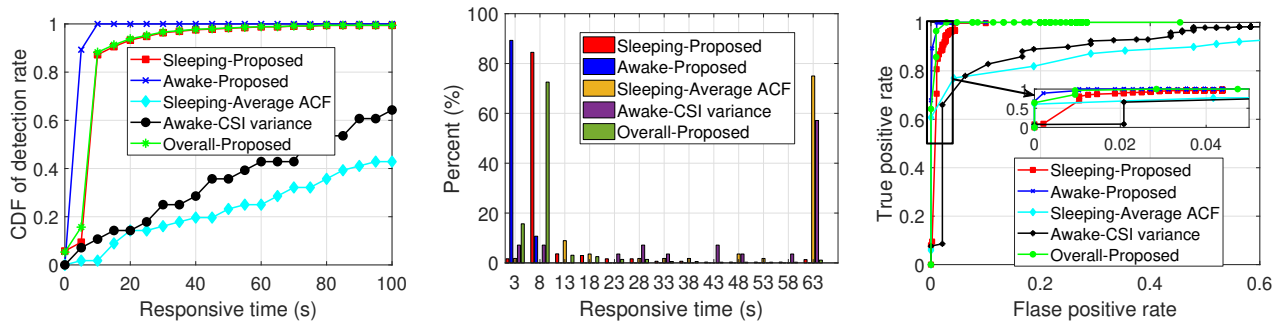

(a) Detection rate (b) Distribution of responsive time (c) ROC curves

Fig. 3: Overall performance of the CPD system.

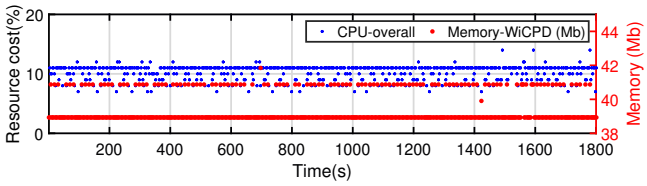

Fig. 4: Resource consumption of the CPD system.

4.1. Overall Performance

Fig. 3 mainly shows the overall detection rate, response time distribution and the Receiver's Operating Characteristic (ROC) of the proposed CPD system. As seen, the proposed system achieves about 100% and 96.56% detection accuracy with the responsive time $\leq$ 8s and $\leq$ 20s for an awake/motion child and sleeping/static child, respectively. Note that we did not show the transition status alone as it is contained in the sleeping/static scenario for most of the time. However, we point out that the overall detection accuracy of the proposed system is about 90.2% without the transition target detector while it raises to 96.87% detection rate when enabling all the three detectors. Fig. 3a also shows that the proposed system takes a longer time to detect a sleeping/static child. This is because that the stationary target detector takes at least longer than one breathing cycle (corresponding to 2-10s) to estimate the breathing rate and the breathing rate has to last continuously for several seconds to confirm that it is motivated by the breathing motion of a child rather than noise or distortions, thus causing a longer delay than the motion target detector. Fig. 3c shows the ROC performance of the proposed system, demonstrating 1.04% and 4.37% false alarm rate for an awake and sleeping child respectively, with the detection rate $\geq$ 99.6%. For comparison, we also implement the benchmark methods using CSI variance to detect motion and the averaged CSI over subcarreris to estimate the breathing rate. As seen in Fig. 3, the proposed system outperforms the benchmark methods in both detection accuracy and response capability. Thus, experiment results depict the superiority of the proposed CPD system.

4.2. Resource Consumption

It is also important to evaluate the overhead of IWCPD to assess its applicability in practice. Towards this goal, we record the resource consumption log provided by *top*[3] command in real-time experiments. Fig. 4 demonstrates the CPU and memory consumption of the proposed system running on a Dual-core ARM Cortex-A7 CPU up to 1GHz. As seen, the proposed system only consumes about 11% of the CPU and 40MB RAM. Note that for demo purpose, we shown both the breathing rate and motion intensity plots in the real time system while we only need to output a binary decision in practice, which can further reduce the CPU and RAM consumption. As a result,in terms of resource consumption, we believe that the proposed CPD system is affordable for most of the existing in-car system.

5. CONCLUSION

This paper presents an intelligent child presence detection system based on the 2.4/5GHz commercial Wi-Fi which can integrate with current in-car system without additional hardware cost while covering the entire car without blind spot. We implement the proposed CPD system and conduct extensive real-world experiments over different car models for both empty case and in detecting children of different ages/weights/genders. The results show that the proposed CPD system can respond timely within 20s by using very cheap CPU and memory consumption while achieving $\geq$ 99.6% detection accuracy with $\leq$ 4.37% false alarm rate regardless of the status and location of the child. Real-time experiments also show that the proposed system is environment independent and can deploy in minutes without calibration, thus showing its great potential in world-wide deployment.

[3] **top** command is typically used to show the usage of CPU, memory, etc.

6. REFERENCES

[1] M. Catherine, N. Jan, and Q. James, "Heat stress from enclosed vehicles: moderate ambient temperatures cause significant temperature rise in enclosed vehicles," *Pediatrics*, vol. 116, no. 1, pp. e109–e112, 2005.

[2] "Heatstroke deaths of children in vehicles." [Oline]. Available at `https://www.noheatstroke.org/original/`, Accessed Mar. 06, 2021.

[3] "Euro NCAP 2025 Roadmap." [Oline]. Available at `https://cdn.euroncap.com/media/30700/euroncap-roadmap-2025-v4.pdf`, Accessed Mar. 06, 2021.

[4] K. N. Khamil, S. Rahman, and M. Gambilok, "Babycare alert system for prevention of child left in a parked vehicle," *ARPN Journal of Engineering and Applied Sciences*, vol. 10, no. 22, pp. 17313–17319, 2015.

[5] N. Hashim, H. Basri, A. Jaafar, M. Aziz, and A. S. A. Ja, "Child in car alarm system using various sensors," *ARPN Journal of Engineering and Applied Sciences*, vol. 9, no. 9, pp. 1653–1658, 2014.

[6] J. Redmon and A. Farhadi, "Yolov3: An incremental improvement," *arXiv preprint arXiv:1804.02767*, 2018.

[7] H. Cai, D. Lee, H. Joonkoo, Y. Fang, S. Li, and H. Liu, "Embedded vision based automotive interior intrusion detection system," in *2017 IEEE International Conference on Systems, Man, and Cybernetics (SMC)*, pp. 2909–2914, IEEE, 2017.

[8] C. Fan, Y. Wang, and C. Huang, "Heterogeneous information fusion and visualization for a large-scale intelligent video surveillance system," *IEEE transactions on systems, man, and cybernetics: systems*, vol. 47, no. 4, pp. 593–604, 2016.

[9] A. Caddemi and E. Cardillo, "Automotive anti-abandon systems: a millimeter-wave radar sensor for the detection of child presence," in *2019 14th International Conference on Advanced Technologies, Systems and Services in Telecommunications (TELSIKS)*, pp. 94–97, 2019.

[10] F. Wang, X. Zeng, C. Wu, B. Wang, and K. J. R. Liu, "Driver vital signs monitoring using millimeter wave radio," *IEEE Internet of Things Journal*, pp. 1–1, 2021.

[11] L. Bell., "Cheap Cars With WiFi Capability." [Oline]. Available at `https://www.autobytel.com/car-buying-guides/features/cheap-cars-with-wifi-capability-130477/`, Accessed Mar. 06, 2021.

[12] F. Zhang, C. Wu, B. Wang, H. Q. Lai, Y. Han, and K. J. R. Liu, "WiDetect: Robust motion detection with a statistical electromagnetic model," *Proceedings of the ACM on Interactive, Mobile, Wearable and Ubiquitous Technologies*, vol. 3, no. 3, pp. 1–24, 2019.

[13] D. A. Hill, "Plane wave integral representation for fields in reverberation chambers," *IEEE Transactions on Electromagnetic Compatibility*, vol. 40, no. 3, pp. 209–217, 1998.

[14] R. K. Pearson, Y. Neuvo, J. Astola, and M. Gabbouj, "Generalized hampel filters," *EURASIP Journal on Advances in Signal Processing*, vol. 2016, no. 1, pp. 1–18, 2016.

[15] D. A. Hill, *Electromagnetic fields in cavities: deterministic and statistical theories*, vol. 35. John Wiley & Sons, 2009.

[16] F. Wang, F. Zhang, C. Wu, B. Wang, and K. J. R. Liu, "Respiration tracking for people counting and recognition," *IEEE Internet of Things Journal*, vol. 7, no. 6, pp. 5233–5245, 2020.

[17] A. E. J. R. Barryand Lee and D. G. Messerschmitt, *Digital communication*. Springer Science & Business Media, 2012.

[18] F. Zhang, C. Wu, B. Wang, M. Wu, D. Bugos, H. Zhang, and K. J. R. Liu, "Smars: Sleep monitoring via ambient radio signals," *IEEE Transactions on Mobile Computing*, vol. 20, no. 1, pp. 217–231, 2021.

[19] G. S. K. C. Veluvolu, "Surface chest motion decomposition for cardiovascular monitoring," *Scientific reports*, vol. 4, no. 1, pp. 1–9, 2014.

[20] X. Zeng, M. Yang, B. Chen, and Y. Jin, "Estimation of direction of arrival by time reversal for low-angle targets," *IEEE Transactions on Aerospace and Electronic Systems*, vol. 54, no. 6, pp. 2675–2694, 2018.

[21] X. Zeng, F. Zhang, B. Wang, and K. J. R. Liu, "Radio frequency based direction sensing using massive mimo," *IEEE Access*, vol. 8, pp. 26827–26838, 2020.

[22] X. Zeng, B. Chen, and M. Yang, "DOA estimation for low angle targets using time reversal in frequency domain model," in *2018 IEEE Radar Conference (RadarConf18)*, pp. 1323–1327, 2018.

[23] S. Fang, R. Alterovitz, and S. Nirjon, "Non-line-of-sight around the corner human presence detection using commodity wifi devices," in *Proceedings of the 1st ACM International Workshop on Device-Free Human Sensing*, pp. 22–26, 2019.